

# PROGRESSIVE FAILURE OF UNSATURATED FILL SLOPE CAUSED BY CUMULATIVE DAMAGE UNDER SEEPAGE SURFACE

\*Hidehiko Murao<sup>1</sup>, Kentaro Nakai<sup>2</sup>, Takahiro Yoshikawa<sup>2</sup> and Toshihiro Noda<sup>2</sup>

<sup>1</sup>Murao Chiken Co., Ltd, Japan; <sup>2</sup> Department of Civil Engineering, Nagoya University, Japan

\*Kentaro Nakai, Received: 23 Nov. 2020, Revised: 16 Dec. 2020, Accepted: 25 Dec. 2020

**ABSTRACT:** Seepage surface position of fill slope can fluctuate owing to rainfall and groundwater supply from behind the slope. Therefore, in this study, shaking-table tests of an unsaturated fill slope were conducted to examine the influence of the seepage surface position on the fill slope stability by comparing with previous results in the fully saturated condition. An acceleration amplification factor was used to evaluate the stability. If the embankment was in an unsaturated condition, a slip plane was formed along the seepage surface. With ongoing increase of input acceleration, the slip progressed to behind the slope. Comparison of the unsaturated and saturated results showed that although the failure mechanism in which the slip surface was formed by the reduction in rigidity was common, the input acceleration at failure and deformation mode were different. When the slip surface was formed and failure occurred, the input acceleration in the unsaturated fill slope was more massive, and the deformation at the same excitation stage was small. These results imply that the unsaturated fill slope has a higher earthquake resistance than the saturated fill slope. Moreover, it is shown that the progress of plastic deformation inside the embankment and the formation process of the slip plane can be estimated from the change in the acceleration amplification factor regardless of seepage surface position.

*Keywords: Unsaturated fill slope, Seepage surface, Progressive failure, Resonance, Shaking-table test*

## 1. INTRODUCTION

As there is limited flat land in Japan, construction methods in which hilly areas are cut down and the resulting soil used to fill nearby valleys or low-lying terrain have been widely adopted. As a result, there are many hillside embankments in Japan, ranging from large to small in scale. These hillside embankments represent a geotechnical risk during earthquakes, and there have indeed been many reports to date of severe damage occurring as a result of significant earthquakes [1 - 3].

The authors previously conducted a series of shaking-table tests to evaluate saturated hillside embankment, to identify the failure and deformation mechanisms of hillside embankments during earthquakes [4]. It was found that the input frequency affected how the model slope moved and the magnitude of acceleration leading to collapse. When the input frequency and the initial natural frequency of the model slope were almost the same, large oscillations due to resonance occurred at the beginning of the initial stage, and the amount of deformation substantially increased compared to other input frequencies. This indicates that the relationship between the natural frequency of the ground and the predominant frequency of the seismic motion is an essential factor determining the seismic stability of hillside embankments, and

thus the stability cannot be determined by the magnitude of acceleration, such as adopted in the conventional seismic coefficient design method.

Another factor that has been found to affect the seismic stability of hillside embankments is the seepage surface position inside the embankment. The groundwater level in a hillside embankment naturally fluctuates according to the supply of groundwater from any rear upslope and rainwater, so it is presumed that the seismic behavior varies depending on the seepage surface position. In fact, among the observations and measurements collected after the collapse of hillside embankments due to earthquakes, many reports are indicating that the groundwater level was high. However, there have also been reports of hillside embankments when the groundwater level was located about halfway up the slope [1, 5]. Therefore, it remains essential to determine the effect of the groundwater level on the seismic behavior of hillside embankments.

Although few in number, model experiments on the behavior of unsaturated embankments during earthquakes have been conducted [6 - 12]. Most of them focus on the position and depth of the seepage surface, and almost no studies have focused on the difference in frequency characteristics of the external force, especially the effect of resonance behavior on the stability of unsaturated embankments during earthquakes. Furthermore,

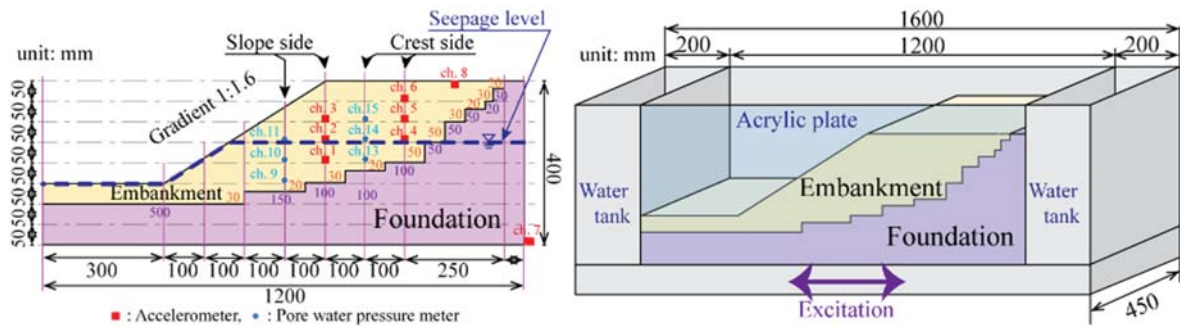


Fig. 1 Dimensions of the model ground and arrangement of the measuring instruments

most of the studies were on unsaturated embankments constructed on the horizontal ground such as river dikes, and there are few studies on hillside embankments, which is the target of this study. Therefore, it would be beneficial to accumulate model test results for the purpose of understanding the effect of seepage surface position of the hillside embankments on their seismic behavior. This study conducted a series of shaking-table tests on embankments in the unsaturated state and compared with previous results in the fully saturated condition [4] to determine the effects of seepage surface position on the stability, deformation modes, and failure mechanisms of hillside embankments during earthquakes.

## 2. TEST CONDITIONS

### 2.1 Overview of the Model Slope

Figure 1 shows the configuration of the rigid soil tank and model slope, instrument installation, and seepage position used in the tests. Note that hereafter, “hillside embankment” refers to a constructed hillside embankment, and “model slope” refers to the 1/50 scale model of a typical hillside embankment consisting of a foundation and embankment. The term “foundation” refers to the bedrock underlying the embankment or model slope, and “embankment” refers to the material atop the foundation. About the similitude rules under 1g field, refer the previous research [4]. The water tanks at the front and rear of the soil tank were used to create the seepage surface in the model slope. The soil samples and method of preparing the model slope were the same as in the previous research [4], except for the seepage surface position. As shown in Fig. 1, seven accelerometers (chs. 1-6 and ch. 8) and seven pore water pressure meters (chs. 9-15) were embedded in the model slope during its construction, with one accelerometer (ch. 7) installed at the bottom of the soil tank to measure the input excitation. All data were collected at a sampling rate of 1,000 Hz. The accelerometers of chs. 1-3 and the pore water pressure meters of chs.

9-11 are referred to as the “slope side”, and the accelerometers of chs. 4-6 and the pore water pressure meters of chs. 13-15 are referred to as the “crest side”.

The particle size distribution of the soil material used in the tests is shown in Fig. 2. The foundation material was Mikawa silica sand (Nos. 4, 5, 5.6, 6, and 7) mixed in proportions of 1:1:1:1:1 by mass, to which a cement-solidification material was added at a rate of 150 kg/m<sup>3</sup>. The elastic modulus obtained from uniaxial compression tests after 28 days of curing was  $E = 450$  MPa. After curing for 28 days, it was formed into a stair shape. Soil cement was used as the foundation material because the bedrock of the fill slopes that have deformed in an earthquake frequently follow the Neogene Series or Pleistocene Series and are relatively stronger than the embankment part [1]. The embankment material was formed by mixing Mikawa silica sand (Nos. 4, 5, 6, and 7), DL clay, and Fujinomori clay in proportions of 3:3:3:3:4:4 by mass which can be classified as silty sand (SM) by unified soil classification system. This was because the embankment material of the fill slopes damaged in the past earthquakes was made up of soil arising from cutting nearby hills and intermediate soil that included fine fractions [1]. The density of the soil was controlled to ensure a degree of compaction  $D_c$

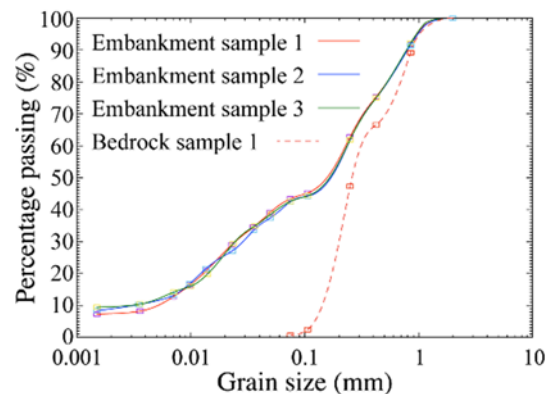


Fig. 2 Particle-size distributions for foundation and embankment material.

= 90% (for a dry density  $\rho_d = 1.72 \text{ g/cm}^3$ ), and the soil was tamped in 15 horizontal layers (each 2 cm thick). After raising the seepage level to about the mid-height of the model slope in stages over for 12 hours, water was allowed to seep at a constant level for 156 hours. Finally, the intended model slope geometry was excavated. Actually, seepage surface would curve downward before meeting the face of the slope. However, precise location of seepage surface near the slope is hard to understand. Therefore, for the purpose of clarity, the seepage surface position before excavation was drawn in the figure. Note that when the seepage level was raised, its location was confirmed using the equivalent static pressure measured by the pore water pressure meters.

## **2.2 Excitation Conditions**

The excitation method employed in this study was the same as that employed in the previous research [4]. A sine wave frequency sweep was performed in advance with a constant acceleration amplitude of  $0.2 \text{ m/s}^2$ . This indicated an initial natural frequency of the unsaturated model slope of approximately 50 Hz, the same as that previously determined for the saturated model slope, confirming that the seepage level does not affect the natural frequency of the model slope. Therefore, the input frequency was determined as 50 Hz, as this was almost the same as the initial natural frequency of the model slope. The excitation acceleration was given by sine waveform with its amplitude increasing from  $0.2 \text{ m/s}^2$  to  $7.7 \text{ m/s}^2$  by  $0.5 \text{ m/s}^2$  increments. In each increment stage, the excitation time was 60 s, and an interval of 240 s was initially provided between each stage in preparation for the next stage. However, virtually no fluctuation in the pore water pressure was observed during this interval; therefore, it was determined that continuous excitation could be applied. Note that all tests were performed several times under the same conditions to confirm reproducibility.

## **2.3 Evaluation Index for Estimating the State Inside the Embankment**

In the previous research [4], in addition to performing observations from the side and top, the formation of slip/discontinuity surfaces inside the embankment was estimated from the acceleration amplification factors measured along the depth direction. The acceleration amplification factor, which is defined by the ratio of the amplified acceleration at each measurement point to the input acceleration, was used in the previous research [4]. If the observed acceleration was not steady and fluctuated during excitation, the acceleration value at the end of each vibration stage was adopted to

calculate the amplification factor. From the previous study, the following characteristics were obtained using the acceleration amplification factor.

- When the embankment was close to its initial condition with no deformation or failure, the acceleration amplification factor at the shallower portion with low constraint pressure became larger compared with the deeper portion with high constraint pressure.
- When the input frequency was close to the natural frequency of the model slope, the amplification factor was increased by the resonance phenomena.
- When the magnitude of the input acceleration was increased and the rigidity of the embankment was decreased by the accumulation of the plastic deformation, the natural frequency of the model decreased and became out of the resonance region. The acceleration amplification factor turned to be decreased at this stage.
- When the magnitude of the input acceleration was further increased, a reduction in rigidity of the embankment finally led to failure, and a discontinuity surface was formed inside the embankment. At this moment, the applied vibration was hard to transmit to portions of the embankment above the discontinuity surface. Therefore, the acceleration amplification factor was decreased at the higher portion and observed to invert along the depth direction.

The state inside the embankment could be estimated by analyzing the acceleration amplification factor. Therefore, following the previous research [4], the internal damage (progression/accumulation of plastic deformation and formation of discontinuity surface) of the embankment was estimated from the acceleration amplification factor. Additionally, the excess pore water pressure ratio (ratio of the excess pore pressure generated by cyclic shear to the initial effective overburden pressure) was used to know the rigidity reduction inside the embankment.

## **3. RESULTS**

Figures 3 and 4 show the changes in the acceleration amplification factor and excess pore water pressure ratio, respectively, with increasing input acceleration. The following phases in the model slope response could be differentiated in the results reported in Figs 3 and 4: resonance, reduction in natural frequency, slip formation and slip progression.

### **3.1 Stages 1 to 3: Resonance**

By comparing the amplification factors along the depth direction shown in Fig. 3, it could be seen that in the initial stages, the amplification factors within the model slope increased as the overburden

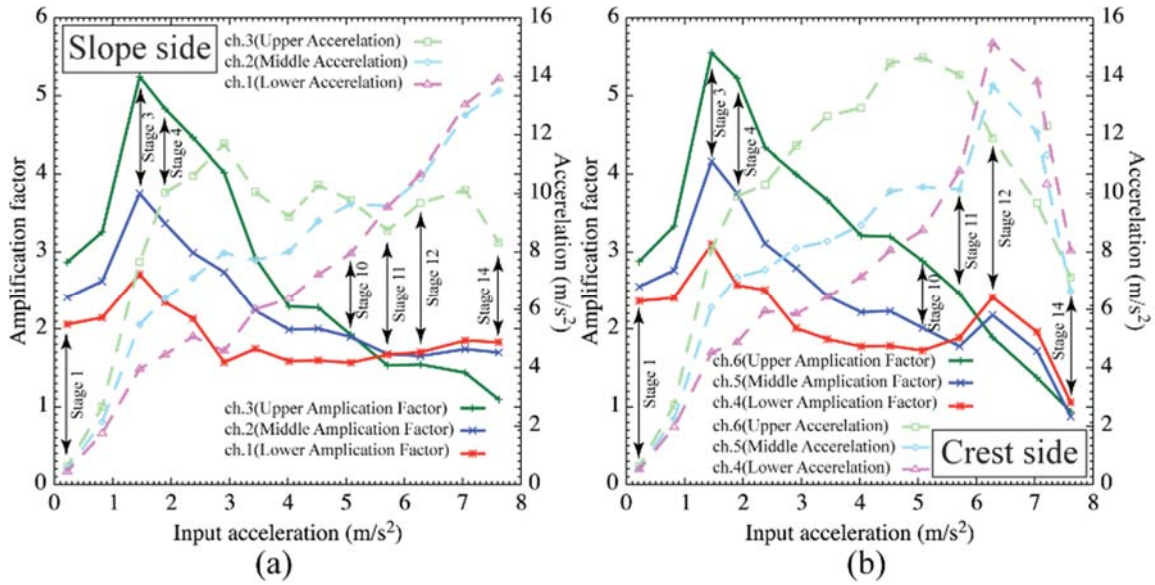


Fig. 3 Relationship between input acceleration and maximum acceleration/acceleration amplification factor on the (a) slope side and (b) crest side of the model slope

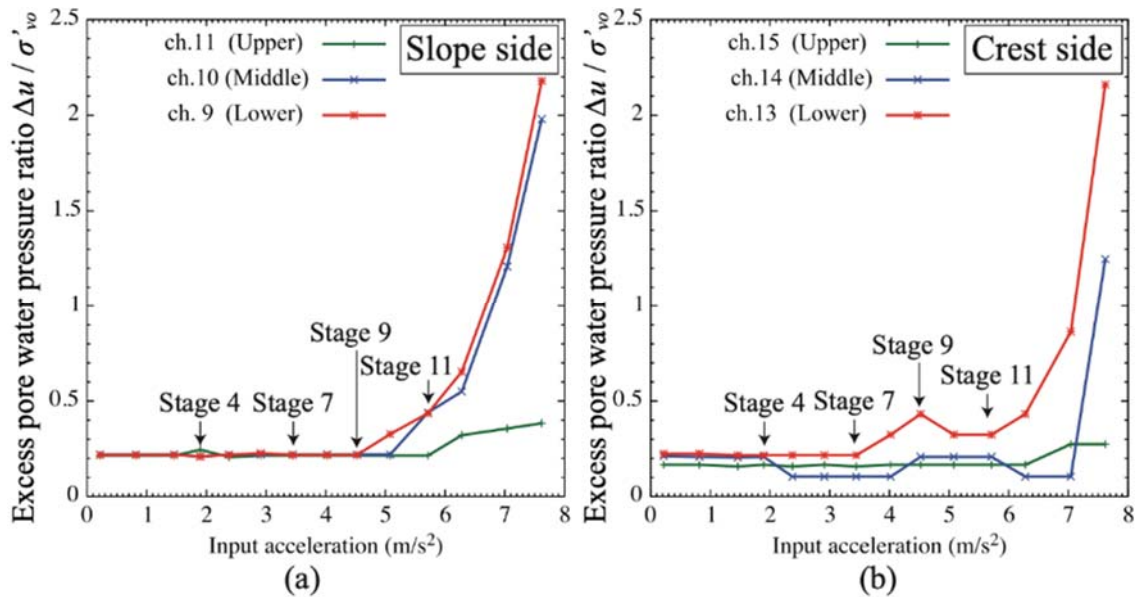


Fig. 4 Relationship between input acceleration and excess pore water pressure ratio on the (a) slope side and (b) crest side of the model slope

pressure decreases, and the entire slope remained close to its initial state. Thus, the amplification factors could be observed to increase for shallower levels on both the slope and crest sides of the model slope. Furthermore, the amplification factor at each level increased as the input acceleration increased, reaching a maximum in Stage 3. At this stage, the input frequency is close to the natural frequency of the model slope, causing a resonance to occur in which the oscillations in the shallow levels of the model slope were more significant than those in the

deep levels. Because resonance occurred in these stages, large oscillations were produced even if the input acceleration was small.

### 3.2 Stages 4 to 9: Reduction in Natural Frequency

When the input acceleration increased in stages 4 to 9, although the accelerations continued to increase at each measurement point in Fig. 3, the amplification factors decreased while maintaining their relative values along the depth direction. There

was a notable reduction in the amplification factor at the upper (chs. 3 and 6) and middle (chs. 2 and 5) levels of the model slope compared with the lower level (chs. 1 and 4). As the acceleration increased, the inertial forces acting on the embankment increased. The amplification factor is thought to decrease from Stage 4 onwards because of the accumulation of plastic deformation due to repeated loading, and because the natural frequency of the model slope decreased, resonance response was eliminated. As the reduction in the amplification factor after Stage 4 was more significant in the upper level where the overburden pressure is small, the progress of plastic deformation was more significant as the constraint pressure decreases at the top of the slope and crest, and near the slope surface. These phenomena are similar to those observed in the previous research [4] and are not considered to depend on the groundwater conditions. However, the measured acceleration value decreased from Stage 7 only at the upper side of the slope. Moreover, reduction in the acceleration amplification factors was more significant on the slope side than on the crest side, which indicates

that the progress of plastic deformation was more prominent on the upper side of the slope.

### 3.3 Stages 10 to 11: Slip Formation Near the Slope Surface

By the time that excitation Stage 10 was completed, the acceleration amplification factors were reversed at the upper (ch. 3) and middle (ch. 2) levels of the embankment on the slope side. Since the excess pore water pressure ratios at the lower (ch. 9) and middle (ch. 10) levels of the model slope began to rise, its rigidity was considered to have significantly decreased, and a discontinuity surface has likely formed in the saturated zone close to the seepage surface, making it difficult to transmit acceleration to the upper levels of the model slope. Figure 5 shows the deformation after Stage 10, as inferred from the measurements and observations. In the figure, slip occurred starting in the vicinity of the seepage surface and was moving toward the middle level of the model slope on the slope side. Note that in Stage 10, there is no change in the magnitude of the amplification factor on the crest

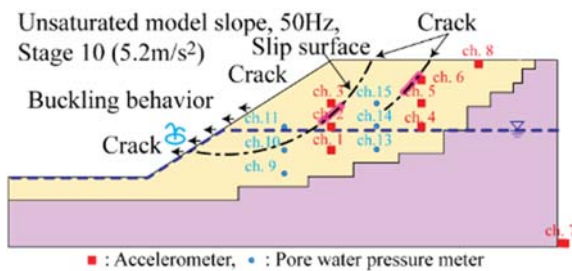


Fig. 5 Deformation within the model slope during Stage 10 excitation

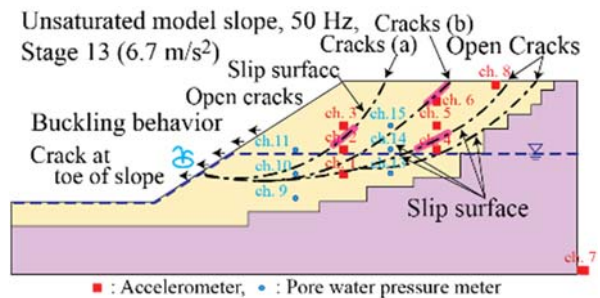


Fig. 6 Deformation within the model slope during Stage 13 of excitation

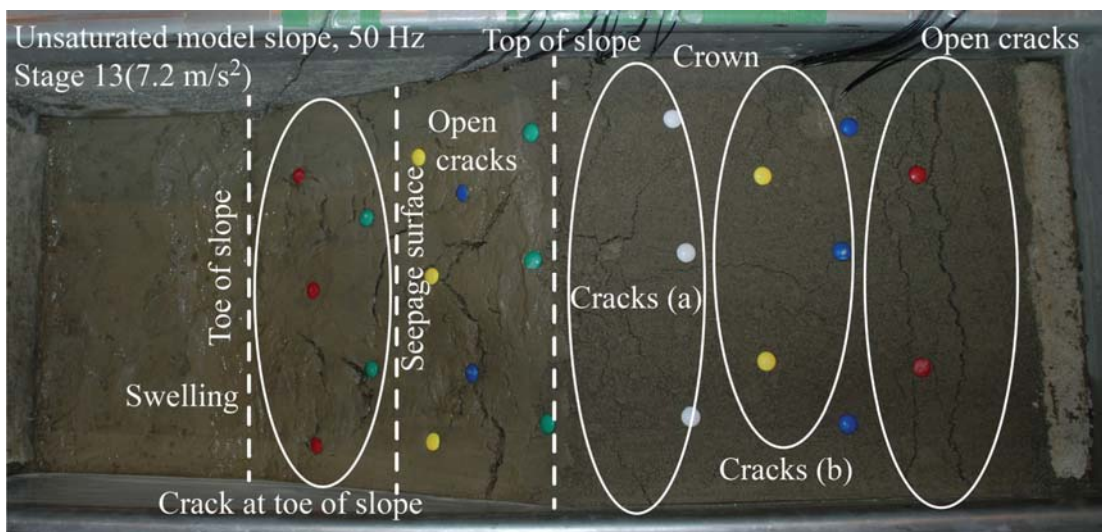


Fig. 7 Top surface of the model slope during Stage 13 of excitation

side, nor is there any change in the excess pore water pressure ratio. Therefore, from stages 10 to 11, it could be seen that a discontinuous surface was first formed near the seepage surface on the slope side, and a thin slip plane near the slope was generated. However, a slip plane on the crest side had not yet been formed at this stage.

### 3.4 Stages 11 to 14: Progressive Failure Toward the Rear (Crest Side) of the Model

After Stage 12, the excess pore water pressure ratio turned to increase even on the crest side at the lower level (ch. 13). Additionally, the amplification factors measured at the middle (ch. 5) and lower (ch. 4) levels, and at the upper (ch. 6) and middle (ch. 5) levels of the model slope inverted. Finally, failure within the model slope was observed to progress backward from near the slope surface to the rear of the model. Inversion of the acceleration amplification factors then progressed on the slope side at the middle (ch. 2) and lower (ch. 1) levels of the model slope. On both the slope and crest sides, the amplification factors increased with increasing depth. However, the lower (ch. 1 and 4) level of the embankment showed small increases in the amplification factor. This is because the significant reduction in rigidity occurred at the bottom of the embankment where a discontinuity surface was formulated.

Figure 6 shows the deformation within the model slope after Stage 13, as inferred from the measurements and observations. Slips originating near the seepage surface gradually progressed backward from near the slope surface to the rear of the model, ultimately resulting in overall failure. The resulting large cracks that formed near the slope surface and crest of the slope, and the measured displacement in the lateral direction, were similar to examples of collapse at the top of hillside embankments found in damage reports after large earthquakes.

Figure 7 shows a view from above the model slope at this time. Cracks could be observed in the slope surface near the seepage level that extended out toward the sides of the slope surface. The top of the oscillating soil mass was deformed, beginning to protrude in the front as if preparing to fall forward. Additionally, the cracks in the crest initially observed in Stage 10 were more prominent, and large open cracks could be observed at the rear of the model after a large oscillation.

In Stage 12, the amplification factors at the lower (ch. 4) and middle (ch. 5) levels of the model slope on the crest side temporarily increased, but turned to decrease during Stage 13 and onwards. This is thought to be the result of cross-sectional changes due to the generation of slip surfaces and deformation propagation, resulting in a temporary

change in the vibration properties of the model slope. At the final stage (Stage 14), the amplification factors on the slope side were determined to be 1.9, 1.7, and 1.1 at the lower (ch. 1), middle (ch. 2), and upper (ch. 3) levels of the model slope, respectively. The amplification factors on the crest side were determined to be 1.1, 0.8, and 0.9 at the lower (ch. 4), middle (ch. 5), and upper (ch. 6) levels of the model slope, respectively. Therefore, the measurement locations could be broadly divided into those at which the amplification factor was about 2.0 (chs. 1 and 2) and those at about 1.0 (chs. 3-6). In this manner, a clear difference in the amplification factor could be observed after the formation of the slip surfaces.

## 4. EFFECT OF SEEPAGE SURFACE POSITION ON THE SEISMIC BEHAVIOR OF HILLSIDE EMBANKMENT

This section compares the results obtained in this study for an unsaturated model slope with those obtained for a saturated model slope in the previous study [4]. Details about the experimental result of a saturated model slope, see the previous study.

For the saturated model slope, an initial crack was identified in the ground surface at an input acceleration of  $1.2 \text{ m/s}^2$ , whereas no cracks were observed until an input acceleration of  $5.2 \text{ m/s}^2$  for the unsaturated model slope. Furthermore, the input acceleration at overall failure was  $5.7 \text{ m/s}^2$  for the saturated model slope and  $6.7 \text{ m/s}^2$  for the unsaturated model slope. Therefore, for hillside embankments in which all conditions were the same except for the groundwater level, seismic stability increased with decreasing seepage surface position in terms of the input acceleration. This observation supports the effectiveness of groundwater drainage works as a countermeasure against earthquakes.

Next, the deformation progression patterns were compared for saturated and unsaturated model slopes. For the saturated model slope as indicated in Fig. 8 (reprinted from [4]), after water emerged from the crest and flow occurred near the surface from the early vibration stage, large slips extending from the embankment slope to the rear of the model progressed from the upper to lower portions as the

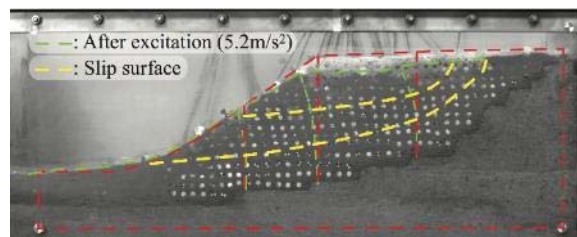


Fig. 8 Deformation within the model slope in case of the saturated condition.

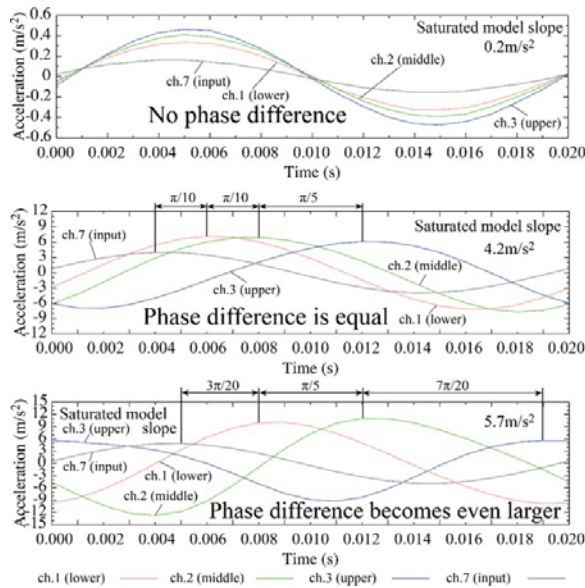


Fig. 9 Phase difference at each level in a saturated model slope

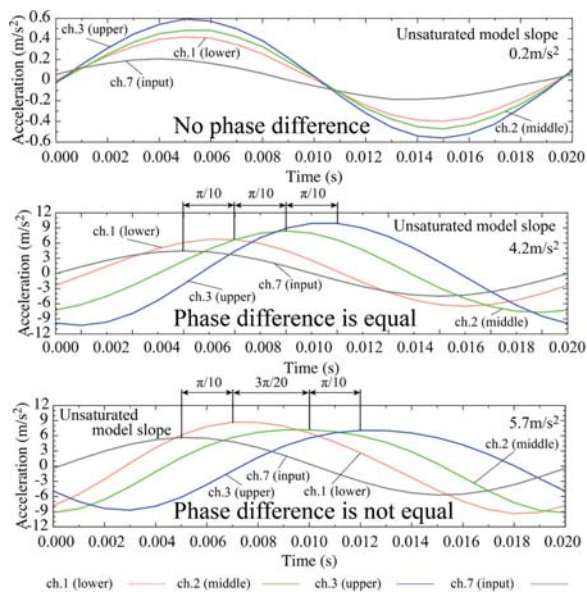


Fig. 10 Phase difference at each depth in an unsaturated model slope

vibration stage increased. For the unsaturated model slope, slips originating at the seepage surface progressed backward from near the slope surface to the rear of the model. However, the discontinuous plane inside the embankment needs larger oscillation to appear as a slip surface on the model surface compared with a saturated embankment. Although the failure was initiated from the shallow saturated zone (seepage surface), the modes of slip and progressive failure within the model slope were observed to differ according to saturation status.

Figures 9 and 10 show the enlargement of the time-acceleration relationship at a specific 1 cycle

of the saturated condition and unsaturated condition respectively. Figure 9 shows the results of the saturated fill slope [4], and Fig. 10 shows the results of the unsaturated fill slope. Three excitation stages were extracted from the data: (1) the initial loading stage, (2) the acceleration stage at which the amplification factors inverted for the first time, and (3) the acceleration stage at which further inversion of the amplification factors occurred. In the initial loading stage, no phase difference could be observed in the acceleration waves regardless of the depth portions for both the saturated and unsaturated model slopes. For the saturated model slope, a significant phase delay could be observed at the upper level of the slope, followed by a phase delay in the middle level, illustrating that disturbance of the soil progressed from the top of the model slope toward its middle. In contrast, for the unsaturated model slope, a phase delay was first observed at the middle level of the slope, suggesting that the disturbance of the soil commenced from near the seepage surface. Therefore, these results are also consistent with the patterns of deformation progression using the acceleration amplification factors described in Section 3.

## 5. CONCLUSIONS

In this study, shaking-table tests were performed on an unsaturated model slope of a typical hillside embankment to identify its deformation mechanisms during an earthquake. The input excitation frequency was set to near the initial natural frequency of the model slope to ensure resonance response. A comprehensive analysis with the previous research using a saturated model slope [4] was then conducted, and the following conclusions were obtained.

1. The initial natural frequency of the unsaturated model slope of approximately 50 Hz, was the same as that of the saturated model, confirming that the seepage surface location does not affect the natural frequency of the model slope.
2. Although the failure initiates from the shallow saturated zone (seepage surface), the failure modes were different according to seepage surface position. The saturated model slope was found that after water emerged from the crest of the slope and flow occurred near the slope surface from the early vibration stage, large slips extended from the embankment slope to the rear of the model, progressing from the upper to lower levels as the vibration stage increased. In contrast, for the unsaturated model slope, slips originating at the seepage surface progressed backward from near the slope surface to the rear of the model.
3. Fill slope in which all conditions were the same except for the groundwater level, seismic

stability increases with decreasing seepage surface position.

4. It was shown that the progress of plastic deformation inside the embankment and the formation process of the slip plane can be estimated from the change of the acceleration amplification factor regardless of seepage surface position.

These conclusions suggest there is a possibility that even if damage occurs to an unsaturated hillside embankment, it may not be visible at the embankment crest. Thus even if there is little or no damage to the buildings or roads atop an embankment after a significant earthquake, the damage could still be progressing inside and could develop into an overall failure due to a subsequent aftershock or separate earthquake. Therefore, from the viewpoint of disaster prevention, even though an unsaturated slope was observed to be relatively safer than a saturated slope, it is essential to note that a slope is not safe just because its groundwater level is low.

In this study, the dimensions of the tank and the embankment material did not intrinsically replicate the actual field conditions. However, advantage of the model experiment is that the soil and boundary conditions are clear, although it might be different from the actual ground. Therefore, the authors are planning to carry out numerical analysis of this model experiment, for example, using the soil-water-air coupled finite deformation analysis. Then, the actual ground is numerically simulated to understand the effects of dimensions of the tank, boundary, fine particle content, suction, etc.

## 6. ACKNOWLEDGMENTS

This research was supported by Grants-in-Aid from the Japan Society for the Promotion of Science (JSPS “Kakenhi” 25249064).

## 7. REFERENCES

- [1] Kamai T., Ohta H., Ban Y. and Murao H., Landslides in urban residential slopes induced by the 2011 off the Pacific coast of Tohoku earthquake, In *Studies on the 2011 Off the Pacific Coast of Tohoku Earthquake*, Springer, Tokyo, 2013, pp. 103-122.
- [2] Japanese Geotechnical Society (JGS), *Great Hanshin-Awaji Earthquake Survey Report*, 1996, pp. 315-322.
- [3] Mori T., Tobita Y. and Okimura T., The damage to hillside embankments in Sendai city during The 2011 off the Pacific Coast of Tohoku Earthquake, *Soils and Foundations*, Vol. 52, No. 5, 2012, pp. 910-928.
- [4] Murao H., Nakai K., Noda T. and Yoshikawa T., Deformation/failure mechanism of saturated fill slopes due to resonance phenomena based on 1 g shaking-table tests, *Canadian Geotechnical Journal*, Vol. 55, No. 11, 2018, pp. 1668-1681.
- [5] Murao H., Kamai T. and Ohta H., Slope disaster in urban residential region by earthquake — Take “the 2011 off the pacific coast of Tohoku earthquake” as an example., *Journal of the Japan Society of Engineering Geology*, Vol. 53, No. 6, 2013, pp. 292-301. [In Japanese.]
- [6] Matsuo O., Saito Y., Sasaki T., Kondoh K. and Sato T., Earthquake-induced flow slides of fills and infinite slopes, *Soils and Foundations*, Vol. 42, No. 1, 2002, pp. 89-104.
- [7] Ichii K., Experimental study on seismic resistance reduction of embankment due to rainfall. *Journal of Earthquake Engineering in Japan Society of Civil Engineering, Division A1: Structural Engineering & Earthquake Engineering*, 28, 2005, pp. 1-8. [In Japanese.]
- [8] Okamura M., Tamamura S. and Yamamoto R., Seismic stability of embankments subjected to pre-deformation due to foundation consolidation, *Soils and Foundations*, Vol. 53, No. 1, 2013, pp. 11-22.
- [9] Higo Y., Lee C.-W., Doi T. Kimura M., Kimoto, S. and Oka, F., Study of dynamic stability of unsaturated embankments with different water contents by centrifugal model tests, *Soils and Foundations*, Vol. 55, No. 1, 2015, pp. 112-126.
- [10] Kominato Y., Matsumaru T. and Sato T., Model shaking table test of unsaturated embankment in different water content. *Journal of Japan Society of Civil Engineering, Division A1: Structural Engineering & Earthquake Engineering*, Vol. 73, No. 4, 2017, pp. 1001-1009. [In Japanese.]
- [11] Ren F., Huang Q. and Wang G., Shaking table tests on reinforced soil retaining walls subjected to the combined effects of rainfall and earthquakes, *Engineering Geology*, Vol. 267, 2020, No. 105475.
- [12] Borghei A., Ghayoomi M. and Turner M., Centrifuge tests to evaluate seismic settlement of shallow foundations on unsaturated silty sand, *Geo-Congress 2020*, 2020, pp. 198-207.